J|A|C|S
ARTICLES
Published on Web 09/04/2004

Structure and Dynamics of Neutral β-H Agostic Nickel Alkyls: A Combined Experimental and Theoretical Study

Elzbieta Kogut,[†] Alexander Zeller,[‡] Timothy H. Warren,*[,†] and Thomas Strassner*[,‡]

Contribution from the Department of Chemistry, Georgetown University, Box 571227, Washington, D.C. 20057-1227 and Department of Inorganic Chemistry, Technical University Munich, Lichtenbergstrasse 4, D-85747 Garching, Germany

Received April 20, 2004; E-mail: thw@georgetown.edu; thomas.strassner@chemie.tu-dresden.de

Abstract: Addition of $BF_3{\cdot}OEt_2$ to ethereal solutions of the Ni(II) β-diketiminates [Me_2NN]Ni(R)(2,4-lutidine) (R = Et (**1**), Pr (**2**)) allows the isolation of the neutral β-H agostic monoalkyls [Me_2NN]Ni(R) (R = Et (**3**), Pr (**4**)). X-ray studies of primary alkyls **3** and **4a** reveal acute Ni−C_α−C_β angles with short Ni−C_β distances, indicating structures along the β-H elimination pathway. Positional disorder of the alkyl group in the X-ray structure of **4** corresponds to partial (22%) occupancy by the secondary alkyl [Me_2NN]Ni($CHMe_2$) (**4b**). Variable-temperature NMR spectra of **3** and **4** reveal fluxional behavior that result from β-H elimination, in-plane rotation of the β-CH_3 group, and a tetrahedral triplet structure for **3** that were investigated by density functional theory calculations at the Becke3LYP/6-31G* level of theory without simplifications on the β-diketiminate ancillary ligand. Calculations support low temperature NMR studies that identify the linear β-H agostic propyl isomer **4a** as the ground state with the branched β-H agostic isomer **4b** slightly higher in energy. NMR studies and calculations show that the β-agostic **3** reluctantly coordinates ethene and that **3** is the ground state for this ethylene oligomerization catalyst. The thermodynamic isotope effect K_H/K_D = 1.3(2) measured for the loss of 2,4-lutidine from **1** to form β-agostic **3** was also examined by DFT calculations.

Introduction

Later transition-metal catalysts for ethylene oligomerization and polymerization have attracted a great deal of attention because of their lower electrophilicity and resulting greater heteroatom tolerance as compared to that of early metal systems.[1−5] An early example is the Shell higher olefin process (SHOP)[6−8] developed by Keim et al., which employs monoanionic O∩P ligands in [Ph_2PC(R)═C(R)O]Ni(Ph)L (L = phosphine) complexes that catalyze the formation of linear α-olefins (C_6−C_{20}) from ethylene in 1,4-butanediol.[9] Later work by Ostoja-Starzewski[10−13] and Klabunde[14,15] showed that replacing the phosphine in SHOP-like catalysts with more weakly coordinating neutral ligands led to similarly heteroatom-tolerant catalysts capable of producing linear, high molecular weight polyethylene.

Seminal work by Brookhart has shown that cationic monoalkyl complexes of nickel and palladium supported by diimine ligands bearing bulky *N*-aryl substituents can lead to very active α-olefin polymerization systems.[16−27] Both the polymerization activity as well as the degree of branching can be tuned by varying the bulk of the *N*-aryl substituents as well as the monomer concentration.[16,19,21,22,28] While associative chain transfer leading

[†] Georgetown University.
[‡] Technical University Munich. Current address: Technical University Dresden, Institute of Organic Chemistry, D-01062 Dresden, Germany.

(1) Britovsek, G. J. P.; Gibson, V. C.; Wass, D. F. *Angew. Chem., Int. Ed.* **1999**, *38*, 428.
(2) Ittel, S. D.; Johnson, J. K.; Brookhart, M. *Chem. Rev.* **2000**, *100*, 1169.
(3) Boffa, L. S.; Novak, B. M. *Chem. Rev.* **2000**, *100*, 1479.
(4) Mecking, S. *Coord. Chem. Rev.* **2000**, *203*, 325.
(5) Mecking, S. *Angew. Chem., Int. Ed.* **2001**, *40*, 534.
(6) Keim, W.; Behr, A.; Limbacker, B.; Kruger, C. *Angew. Chem., Int. Ed. Engl.* **1983**, *22*, 503.
(7) Keim, W.; Appel, R.; Gruppe, S.; Knoch, F. *Angew. Chem., Int. Ed. Engl.* **1987**, *26*, 1012.
(8) Nomura, K. *Recent Res. Dev. Pure Appl. Chem.* **1998**, *2*, 473.
(9) Vogt, D. In *Aqueous-Phase Organometallic Chemistry*; Cornils, B., Herrmann, W. A., Eds.; Wiley-VCH: Weinheim, Germany, 1998; p 541.
(10) Ostoja-Starzewski, K. A.; Witte, J. *Angew. Chem., Int. Ed. Engl.* **1985**, *24*, 599.
(11) Ostoja-Starzewski, K. A.; Witte, J. *Angew. Chem., Int. Ed. Engl.* **1987**, *26*, 63.
(12) Ostoja-Starzewski, K. A.; Witte, J. In *Transition Metal Catalyzed Polymerizations: Ziegler−Natta and Metathesis Polymerization*; Quirk, R. P., Ed.; Cambridge University Press: Cambridge, 1988; p 472.
(13) Ostoja-Starzewski, K. A.; Witte, J.; Reichert, K. H.; Vasiliou, G. In *Transition Metals and Organometallics as Catalysts for Olefin Polymerization*; Kaminsky, W., Sinn, H., Eds.; Springer: Berlin, 1998; p 349.
(14) Klabunde, U.; Ittel, S. D. *J. Mol. Catal.* **1987**, *41*, 123.
(15) Klabunde, U.; Mülhaupt, R.; Herskovitz, T.; Janowicz, A. H.; Calabrese, J.; Ittel, S. D. *J. Polym. Sci., Part A: Polym. Chem.* **1987**, *25*, 1989.
(16) Johnson, L. K.; Killian, C. M.; Brookhart, M. *J. Am. Chem. Soc.* **1995**, *117*, 6414.
(17) Johnson, L. K.; Mecking, S.; Brookhart, M. *J. Am. Chem. Soc.* **1996**, *118*, 267.
(18) Killian, C. M.; Tempel, D. J.; Johnson, L. K.; Brookhart, M. *J. Am. Chem. Soc.* **1996**, *118*, 11664.
(19) Killian, C. M.; Johnson, L. K.; Brookhart, M. *Organometallics* **1997**, *16*, 2005.
(20) Svejda, S. A.; Johnson, L. K.; Brookhart, M. *J. Am. Chem. Soc.* **1999**, *121*, 10634.
(21) Svejda, S. A.; Brookhart, M. *Organometallics* **1999**, *18*, 65.
(22) Gates, D. P.; Svejda, S. A.; Onate, E.; Killian, C. M.; Johnson, L. K.; White, P. S.; Brookhart, M. *Macromolecules* **2000**, *33*, 2320.
(23) Tempel, D. J.; Johnson, L. K.; Huff, R. L.; White, P. S.; Brookhart, M. *J. Am. Chem. Soc.* **2000**, *122*, 6686.
(24) Shultz, L. H.; Tempel, D. J.; Brookhart, M. *J. Am. Chem. Soc.* **2001**, *123*, 11539.
(25) Shultz, L. H.; Brookhart, M. *Organometallics* **2001**, *20*, 3975.
(26) Leatherman, M. D.; Svejda, S. A.; Johnson, L. K.; Brookhart, M. *J. Am. Chem. Soc.* **2003**, *125*, 3068.
(27) Brookhart, M.; Johnson, L. K.; Killina, C. M.; Arthur, S. D.; Feldman, J.; McCord, E. F.; McLain, S. J.; Kreutzer, K. A.; Nennet, A. M. A.; Feldman, J.; Coughlin, E. B.; Ittel, S. D.; Parthasarathy, A.; Tempel, D. J. WO Patent Application 9830609 to DuPont, priority date 1995.

10.1021/ja0477221 CCC: $27.50

to low molecular weight polymers is significantly attenuated by bulky *N*-aryl substituents, facile β-H elimination/reinsertion leads to branched polymers and competes with ethylene insertion into the M−C bond by "chain-walking".

Spectroscopic[16,20,23−26,29] and computational[30−34] studies have shown that the resting state of the cationic Ni- and Pd-based diimine monoalkyl catalysts is either an alkyl−olefin complex or a β-H agostic species, but that these are in equilibrium with one another. In the polymerization of ethylene, Brookhart has shown that the resting state is an alkyl−ethylene complex while in the case of the more sterically demanding propylene monomer, a pseudo three-coordinate β-agostic structure is favored.[20] The dominance of a β-H agostic resting state with α-olefins requires that chain growth becomes first-order in olefin, resulting in significantly lower TOFs than those observed with ethylene. A β-H agostic resting state can also lead to a significant inverse isotope effect in the ethylene polymerization because of a smaller zero-point energy difference in the ground state. This was proposed on the basis of labeling studies in a cationic Co(III) system ($k_H/k_D = 0.48$)[35] and could be confirmed by DFT calculations.[36]

While a great deal of structural and solution dynamic information has been collected for cationic diimine systems, corresponding neutral Ni−monoalkyls have been much less studied, despite the development of several productive catalyst systems with monoanionic O∩N and N∩N donors.[37−45] We recently reported the synthesis of four-coordinate nickel−monoalkyl complexes [Me_2NN]Ni(R)(2,4-lutidine) (R = Me, Et (**1**), Pr (**2**)) supported by the β-diketiminate ligand [Me_2NN]$^-$ derived from 2,4-bis(2,6-dimethylphenylimido)pentane.[46] Variable temperature ^{1}H NMR spectra of these square-planar monoalkyls in toluene-d_8 indicated that the 2,4-lutidine base was labile and, in the case of the β-H containing species, identified an equilibrium with the lutidine-free species [Me_2NN]Ni(R) (R = Et (**3**), Pr (**4**)). The upfield ^{1}H NMR shifts for the β-H atoms in **3** at δ −5.3 ppm as well as two broad signals at δ −2.7 and −7.3 ppm for two isomers of **4** strongly suggested β-H agostic interactions in these species. While a few late metal

Scheme 1. Reversible Loss of Lutidine from **1**

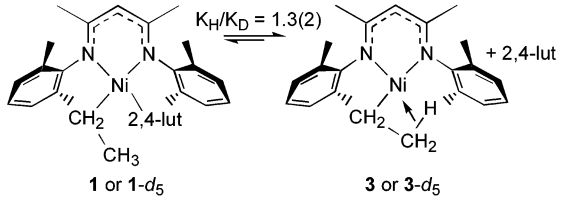

cationic β-H agostic alkyl complexes have been structurally characterized, such as Spencer's [($Bu^t_2PCH_2CH_2PBu^t_2$)Ni(CH_2-CH_3)]$^+$ and [Cp*Co(P(*o*-tolyl)$_3$)(CH_2CH_3)]$^+$,[47,48] structural examples of such neutral complexes are limited to early metal systems such as $TiCl_3Et$(dmpe)[49,50] and [P_2N_2]Ta(CH_2CH_2)Et ([P_2N_2] = PhP($CH_2SiMe_2NSiMe_2CH_2$)$_2$PPh).[51] Herein we report our successful efforts at isolating the lutidine-free species **3** and **4**, their structural and spectroscopic characterization, as well as high-level density functional theory calculations that provide insight into their structure and reactivity.

Results and Discussion

To further probe the β-agostic nature of lutidine-free **3**, we prepared [Me_2NN]Ni(CD_2CD_3)(2,4-lutidine) (**1-*d*$_5$**) employing CD_3CD_2MgI, which allowed us to determine the thermodynamic isotope effect K_H/K_D = 1.3(2) at 25 °C in toluene-d_8 by comparing lutidine dissociation from **1** and **1-*d*$_5$** (Scheme 1). A similar value (K_H/K_D = 1.7) has previously been reported for the equilibrium between the cationic cobalt(III) alkyl [Cp*Co(P(OMe_3)$_3$(CH_2CH_3)(2-fluoropyridine)]$^+$ that dissociates 2-fluoropyridine to give the spectroscopically characterized β-H agostic [Cp*Co(P(OMe_3)$_3$)(CH_2CH_3)]$^+$.[35] Such thermodynamic isotope effects are expected in agostic systems because of the lower C−H(D) vibrational frequencies of the agostic bond relative to the terminal bond leading to the preference of a C−H bond over a C−D bond in an agostic position.[36]

Chemical removal of lutidine from red-orange **1** and **2** by addition of ca. 1.5 equiv BF_3(etherate) in ether results in a cloudy solution that fades to light yellow. Removal of solvent and extraction with pentane allows the isolation of yellow crystals of the base-free β-agostic complexes [Me_2NN]Ni(R) (R = C_2H_5 (**3**); C_3H_7 (**4**)) in about 50% yield, their isolation somewhat hampered by their extreme solubility in hydrocarbons (Scheme 2).[52,53]

The X-ray structures of **3** and **4** reveal square-planar Ni centers with Ni−alkyl groups for which two sets of positions each could be refined. The major site occupancies **3a** (83%) and **4a** (78%) contain primary β-H agostic alkyl groups, illustrated in Figures 1 and 2. The Ni−C23A (C_β) distance of

(28) Guan, Z.; Cotts, P. M.; McCord, E. F.; McLain, S. F. *Science* **1999**, *283*, 2059.
(29) Tempel, D. J.; Brookhart, M. *Organometallics* **1998**, *17*, 2290.
(30) Deng, L.; Margl, P.; Ziegler, T. *J. Am. Chem. Soc.* **1997**, *119*, 1094.
(31) Stromberg, S.; Zetterberg, K.; Siegbahn, P. E. M. *J. Chem. Soc., Dalton Trans.* **1997**, 4147.
(32) Musaev, D. G.; Froese, R. D. J.; Morokuma, K. *Organometallics* **1998**, *17*, 1850.
(33) Woo, T. K.; Ziegler, T. *J. Organomet. Chem.* **1999**, *591*, 204.
(34) Tomita, T.; Takahama, T.; Sugimoto, M.; Sakaki, S. *Organometallics* **2002**, *21*, 4138.
(35) Tanner, M. J.; Brookhart, M.; DeSimone, J. M. *J. Am. Chem. Soc.* **1997**, *119*, 7617.
(36) Zeller, A.; Strassner, T. *Organometallics* **2002**, *21*, 4950.
(37) Johnson, L. K.; Bennett, A. M. A.; Ittel, S. D.; Wang, L.; Parthasarathy, A.; Hauptman, E.; Simpson, R. D.; Feldman, J.; Coughlin, E. B. WO Patent Application 9830609 to DuPont, priority date Jan 4, 1997.
(38) Bansleben, D. A.; Friedrich, S. K.; Younkin, T. R.; Grubbs, R. H.; Wang, C.; Li, R. T. WO Patent Application 9842664 to W. R. Grace & Co., priority date March 24, 1997.
(39) Wang, C.; Freidrich, S.; Younkin, T. R.; Li, R. T.; Grubbs, R. H.; Bansleben, D. A.; Day, M. W. *Organometallics* **1998**, *17*, 314.
(40) Domhöver, B.; Kläui, W.; Kremer-Aach, A.; Bell, R.; Mootz, D. *Angew. Chem., Int. Ed.* **1998**, *37*, 3050.
(41) Kläui, W.; Bongards, J.; Reiss, G. J. *Angew. Chem., Int. Ed.* **2000**, *39*, 3894.
(42) Hicks, F. A.; Brookhart, M. *Organometallics* **2001**, *20*, 3217.
(43) Hicks, F. A.; Jenkins, J. C.; Brookhart, M. *Organometallics* **2003**, *22*, 3533.
(44) Jenkins, J. C.; Brookhart, M. *Organometallics* **2003**, *22*, 250.
(45) Connor, E. F.; Younkin, T. R.; Henderson, J. I.; Waltman, A. W.; Grubbs, R. H. *Chem. Commun.* **2003**, 2272.
(46) Wiencko, H. L.; Kogut, E.; Warren, T. H. *Inorg. Chim. Acta* **2003**, *345*, 199.
(47) Conroy-Lewis, F. M.; Mole, L.; Redhouse, A. D.; Litsler, S. A.; Spencer, J. L. *Chem. Commun.* **1991**, 1601.
(48) Cracknell, R. B.; Orpen, A. G.; Spencer, J. L. *Chem. Commun.* **1984**, 326.
(49) Dawoodi, Z.; Green, M. L. H.; Mtetwa, V. S. B.; Prout, K. *Chem. Commun.* **1982**, 802.
(50) Dawoodi, Z.; Green, M. L. H.; Mtetwa, V. S. B.; Prout, K.; Shultz, A. J.; Williams, J. M.; Koetzle, T. F. *J. Chem. Soc., Dalton Trans.* **1986**, 1629.
(51) Fryzuk, M. D.; Johnson, S. A.; Rettig, S. J. *J. Am. Chem. Soc.* **2001**, *123*, 1602.
(52) The synthesis and X-ray structure of the neutral β-agostic species **3** and **4a** have been presented: Warren, T. H.; Wiencko, H. L.; Kogut, E.; Dai, X.; McDermott, J. International Symposium on Olefin Metathesis, Cambridge, MA, August 2001.
(53) After this methodology was initially presented, Brookhart used a similar approach to generate solutions of neutral β-agostic Ni−Et and Ni−Pr complexes supported by anilinotroponate ligands. We thank the authors for communication of their work prior to publication: Jenkins, J. C.; Brookhart, M. *J. Am. Chem. Soc.* **2004**, *126*, 5827.

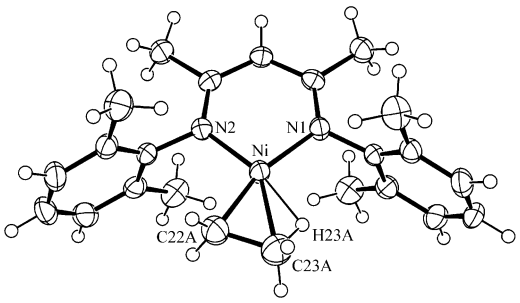

Figure 1. ORTEP diagram of the solid-state structure of **3** (ethyl group in site of 83% occupancy). Selected bond distances (Å) and angles (deg): Ni−N1 1.892(3), Ni−N2 1.859(3), Ni−C22A 1.890(5), Ni−C23A 2.110(6), Ni−H23A 1.66*, C22A−C23A 1.489(6), N1−Ni−N2 97.44(12), Ni−C22A−C23A 76.3(3). (* β-CH_3 H-atoms placed in idealized positions based on riding model.)

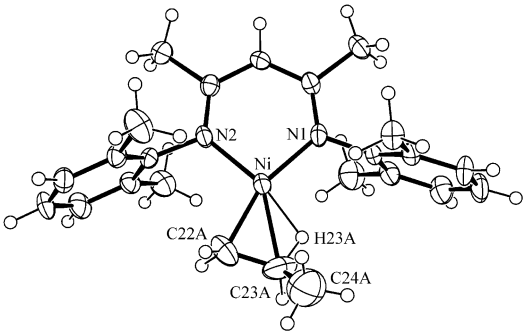

Figure 2. ORTEP diagram of the solid-state structure of **4a** (propyl group in site of 78% occupancy). Selected bond distances (Å) and angles (deg): Ni−N1 1.882(2), Ni−N2 1.870(2), Ni−C22A 1.900(4), Ni−C23A 2.111(5), Ni−H23A 1.61*, C22A−C23A 1.387(6), C23A−C24A 1.544(6), N1−Ni−N2 97.49(10), Ni−C22A−C23A 78.1(3). (* β-CH_2 H-atoms placed in idealized positions.)

Scheme 2. Synthesis of β-Agostic Alkyls [Me_2NN]Ni(R) (R = C_2H_5 (**3**), C_3H_7 (**4**))

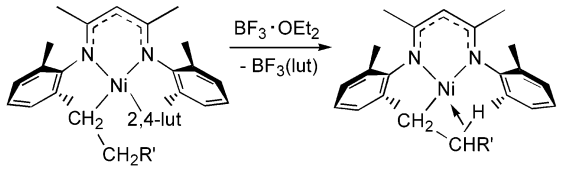

2.110(6) Å in **3a** [2.111(5) Å in **4a**] is only ca. 0.2 Å longer than the Ni−C22A (C_α) distance of 1.890(5) Å in **3a** [1.900(4) Å **4a**], which results in distinctly acute Ni−C22A−C23A angles (**3a**: 76.3(3), **4a**: 78.1(3)). The β-diketiminato Ni−N1 and Ni−N2 distances (**3a**: 1.892(3) and 1.859(3)Å, **4a**: 1.882(2) and 1.870(2) Å) are also contracted relative to those in the corresponding alkyl−lutidine complexes (**1**: 1.915(3), 1.987(3) Å; **2**: 1.919(2), 1.972(2) Å), consistent with a lower coordination number at nickel. Fitting the β-H atoms of **3a** (riding model) and **4a** to idealized positions results in short Ni−H23A distances of 1.66 and 1.61 Å, respectively, consistent with β-H agostic interactions. While not crystallographically observed for **3a**, a shortened $C_\alpha-C_\beta$ distance of 1.387(6) Å in **4a** relative to the $C_\alpha-C_\beta$ distance in nonagostic **2** (1.518(6) Å) suggests a buildup of sp^2 character in the C_α and C_β atoms of the β-agostic alkyl group. Similar Ni−C_α (1.940 and 2.078 Å) and $C_\alpha-C_\beta$ distances (1.435 Å) are found in Spencer's β-agostic cation $[(Bu^t_2PCH_2CH_2PBu^t_2)Ni(CH_2CH_3)]^+$,[47] though the unusually short $C_\alpha-C_\beta$ distance in **4a** may be an artifact of the disorder within the Ni−propyl group (see below). Contracted $C_\alpha-C_\beta$ distances indicate progress along a pathway toward complete β-hydride elimination, which was investigated by DFT calculations discussed later.

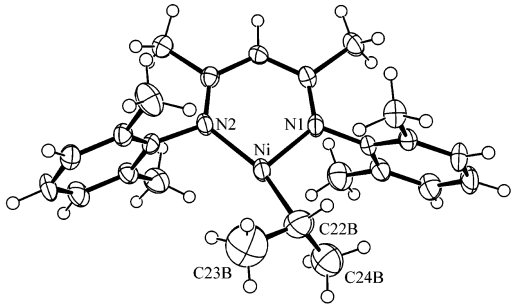

Figure 3. ORTEP diagram of the solid-state structure of **4b** (propyl group in site of 22% occupancy; [Me_2NN]Ni framework unchanged). Selected bond distances (Å) and angles (deg): Ni−C22B 1.865(18), Ni···C23B 2.66, Ni···C24B 2.77.

While the minor occupancy observed in the X-ray structure of **3** is also a primary β-agostic ethyl group in which the C_α is on the opposite side of the β-diketiminato coordination wedge (i.e., trans to N2 instead of N1), the minor occupancy refined in the X-ray structure of **4** is actually the secondary alkyl [Me_2-NN]Ni($CHMe_2$) (**4b**) (Figure 3). Although bond distances within the Ni−$CHMe_2$ moiety of **4b** should be viewed with caution because of its low site occupancy (22%), the Ni−C22B distance of 1.865(18) Å is comparable to the Ni−C22A distances in both **3a** and **4a**. The geometry of **4b** is "bent trigonal" for which the N1−Ni−C22B angle of 154.1(6)° is conspicuously more obtuse than the N2−Ni−C22B angle of 104.0(6)°, a distortion also observed in the related three-coordinate d^9 and d^{10} lutidine adducts [Me_2NN]M(2,4-lutidine) (M = Ni,[54] Cu[55]). In the solid state the isopropyl group of **4b** is not agostic, however, as the long Ni···C23B and Ni···C24B separations (2.66 and 2.77 Å) as well as the closest Ni···H_α (2.36 Å) and Ni···H_β (2.50 Å) contacts for H-atoms placed in idealized positions are well outside of the sum of the corresponding van der Waals radii (Ni−C 2.35 Å; Ni−H 1.85 Å).

Low temperature ^{1}H NMR spectra (500 MHz, −80 °C) of **3** in toluene-d_8 are consistent with its solid-state structure. Two signals are observed for each β-diketiminato *N*-aryl *o*-Me and backbone Me groups, indicating one mirror plane. While the Ni−ethyl α-CH_2 appears as a sharp quartet at δ 0.02 ppm, two broad resonances at δ −1.0 and −14.1 ppm of respective relative areas 2 and 1 are observed for the nonagostic and agostic hydrogen atoms of the β-CH_3 group, which indicates that C−C rotation is almost frozen out. The coalescence temperature of these two upfield resonances of −50(5) °C allows us to estimate the activation barrier to methyl group rotation as $\Delta G^\ddagger = 8.5(5)$ kcal/mol at this temperature, similar to the value of 8.7 kcal/mol reported at −85 °C for a cationic diimine-based β-H agostic Ni−ethyl complex.[26] In addition, a separate fluxional process is observed that interconverts each set of *N*-aryl *o*-Me and backbone Me signals with an activation barrier $\Delta G^\ddagger = 14.9(2)$ kcal/mol at 15 °C. The coalescence temperature for this fluxional process in **3-d_5** is unaffected by isotopic substitution and thus possesses a neglible kinetic isotope effect (k_H/k_D). Furthermore, both the α-CH_2 and β-CH_3 ^{1}H resonances begin to broaden

(54) Wiencko, H. L.; Warren, T. H. 2001, Unpublished observations.
(55) Amisial, L. D. Masters Thesis, Georgetown University, 2003.

Scheme 3. β-H Elimination/Reinsertion Reaction (via $\mathbf{5_{TS}}$) and Symmetrization (via $\mathbf{7_{TS}}$) of **3** (B3LYP/6-31G(d) Free-Energy Values at 298.15 K/1 atm in Kilocalories per Mole)

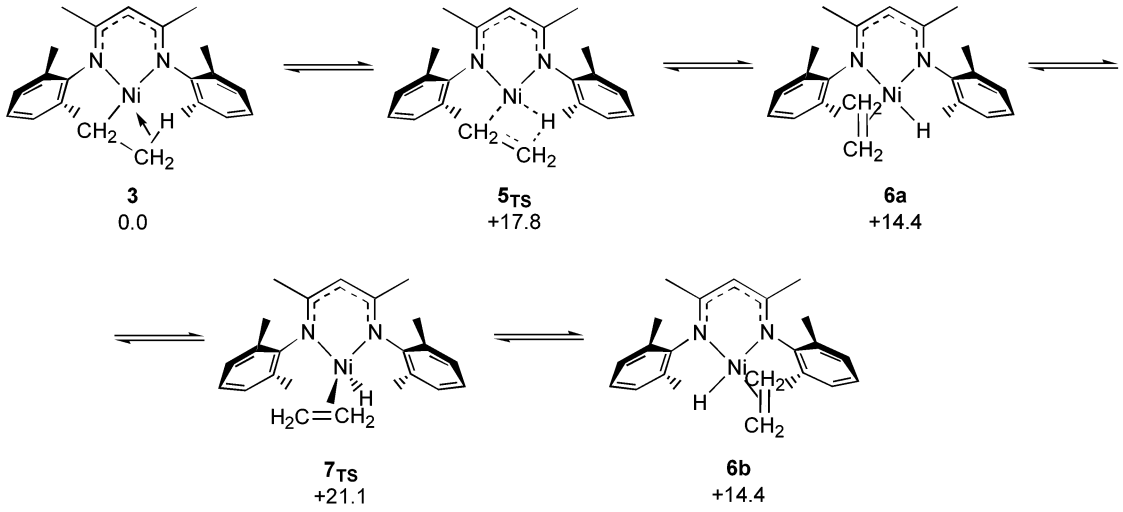

above 15 °C, suggesting an exchange of H atoms between these two sites.

Use of the α-labeled $CH_3{}^{13}CH_2MgI$ in the synthesis of $[Me_2NN]Ni(CH_2CH_3)$(2,4-lutidine) (**1**) leads to equal incorporation of the ^{13}C-label into both positions of the Ni−ethyl group, demonstrating that β-H elimination/reinsertion occurs on the chemical time scale. At −40 °C, these ^{13}C NMR signals appear at δ 8.84 (C_α) and 13.84 (C_β) ppm with coupling constants $^1J_{CH}$ of 128.1 and 124.7 Hz, respectively. Preparing **3** from this labeled material allows the clear assignment of the ^{13}C NMR signals (−40 °C) of the ethyl C_α and C_β atoms at δ 16.10 and 1.40 ppm that have coupling constants $^1J_{CH}$ = 152.7 and 121.4 Hz, respectively. Compared to those in **1**, these coupling constants suggest considerable sp^2 character in the α-CH_2 unit of **3**, and the single β-CH_3 coupling constant likely results from an average of two "alkene-like" and one agostic $^1J_{CH}$ values.[56] Broadening of the C_α and C_β $^{13}C\{^1H\}$ resonances of **3** begins to occur at 20 °C, and these two signals finally coalesce at 75(3) °C (Figure 4). We ascribe this behavior to reversible β-H elimination/reinsertion for which an activation barrier $\Delta G^\ddagger$ = 15.1(3) kcal/mol was determined, just slightly higher than that determined in a related cationic diimine system (14.0 kcal/mol at 6 °C).[26]

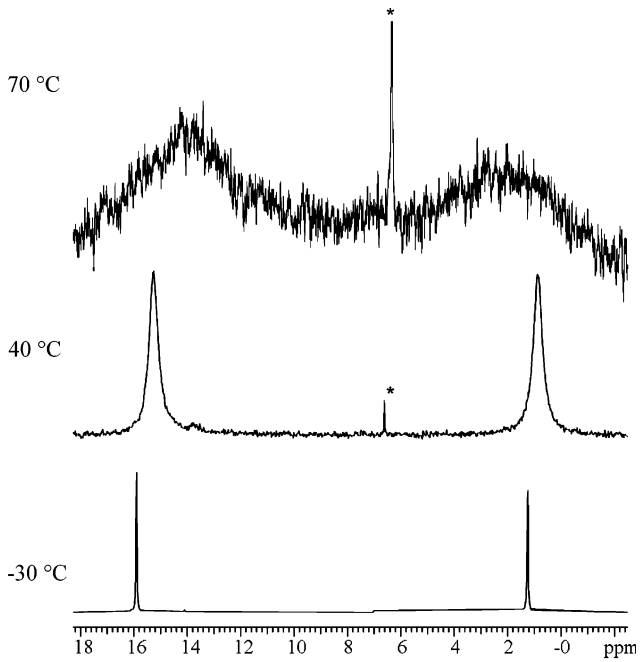

Figure 4. Variable temperature $^{13}C\{^1H\}$ NMR spectra (75 MHz) of the Ni−CH_2CH_3 region of **3** prepared using the ^{13}C-labeled reagent $CH_3{}^{13}CH_2MgI$. The coalescence temperature for the two resonances is 75(3) °C. (* denotes a minor impurity appearing at higher temperatures.)

The very similar barriers to symmetrization in the ^{1}H and ^{13}C NMR experiments suggested the possibility of a common intermediate responsible for the observed spectroscopic behavior. A negligible kinetic isotope effect k_H/k_D was identified by ^{1}H NMR coalescence temperatures of the β-diketiminato *N*-aryl groups, which are identical for both **3** and **3-*d*$_5$**. On the other hand, H_α and β-exchange via H_β elimination/reinsertion should show a significant KIE. This contradiction initiated the investigation by DFT calculations. These were performed on the Becke3LYP/6-31G(d) level of theory without simplifications to the ancillary β-diketiminate ligand.

First the β-H elimination/reinsertion reaction of the β-agostic complex **3** was studied as shown in Scheme 3. Important geometrical parameters for the structures are given in Table 1; three-dimensional representations appear in Figure 5.

The calculated structure of **3** (Figure 5) is in good agreement with the structure obtained from X-ray structural analysis confirming that the chosen level of theory is appropriate. In addition, the position of the β-agostic H-atom could be determined by calculation for which large uncertainties are present when determined by X-ray diffraction. Further illustrating its β-H agostic nature, the LUMO+1 calculated for **3** contains an antibonding interaction between a β-C−H bond and the Ni d-orbital destabilized by σ-donation by the β-diketiminate *N*-donors.[57] Accordingly, the C23−H23A bond is stretched to 1.16 Å, and the Ni−H23A distance is 1.68 Å. During the course of the β-H elimination reaction, the C22−C23 fragment bends out of the Ni-ligand plane. In the transition state $\mathbf{5_{TS}}$, there is a

(56) Brookhart, M.; Green, M. L. H.; Wong, L.-L. *Prog. Inorg. Chem.* **1988**, *36*, 1.
(57) Contour plots of the frontier molecular orbitals may be found in the Supporting Information.

Table 1. Geometric Parameters (Å and deg) for Calculated Structures **3**−**9**[a]

	3	$\mathbf{5_{TS}}$	**6**	$\mathbf{7_{TS}}$	$\mathbf{8_{TS}}$	**9**
Ni−N1	1.91 [1.892(3)]	1.90	1.88	1.92	1.88	1.92
Ni−N2	1.84 [1.859(3)]	1.92	1.96	1.92	1.82	1.91
Ni−C22	1.87 [1.890(5)]	1.96	2.00	1.93	1.87	1.96
Ni−C23	2.12 [2.110(6)]	1.98	2.00	1.93	2.39	3.03
Ni−H23A	1.68 [1.66]	1.42	1.44	1.41	2.52	−
C23−H23A	1.16 [0.98]	1.91	2.30	2.29	1.10	−
C22−C23	1.50 [1.489(6)]	1.41	1.39	1.43	1.54	1.53
N1−Ni−N2	98.3 [97.44(12)]	96.7	95.7	96.6	99.4	97.6
Ni−C22−C23	77.3 [76.3(3)]	69.6	69.5	68.3	88.8	119.8
N2−Ni−C22−C23	−180.0 [−177.2]	155.9	94.6	166.2	180.0	89.2

[a] B3LYP/6-31G(d). Results from X-ray analysis of **3** (ethyl group in site of major occupancy) are given in brackets.

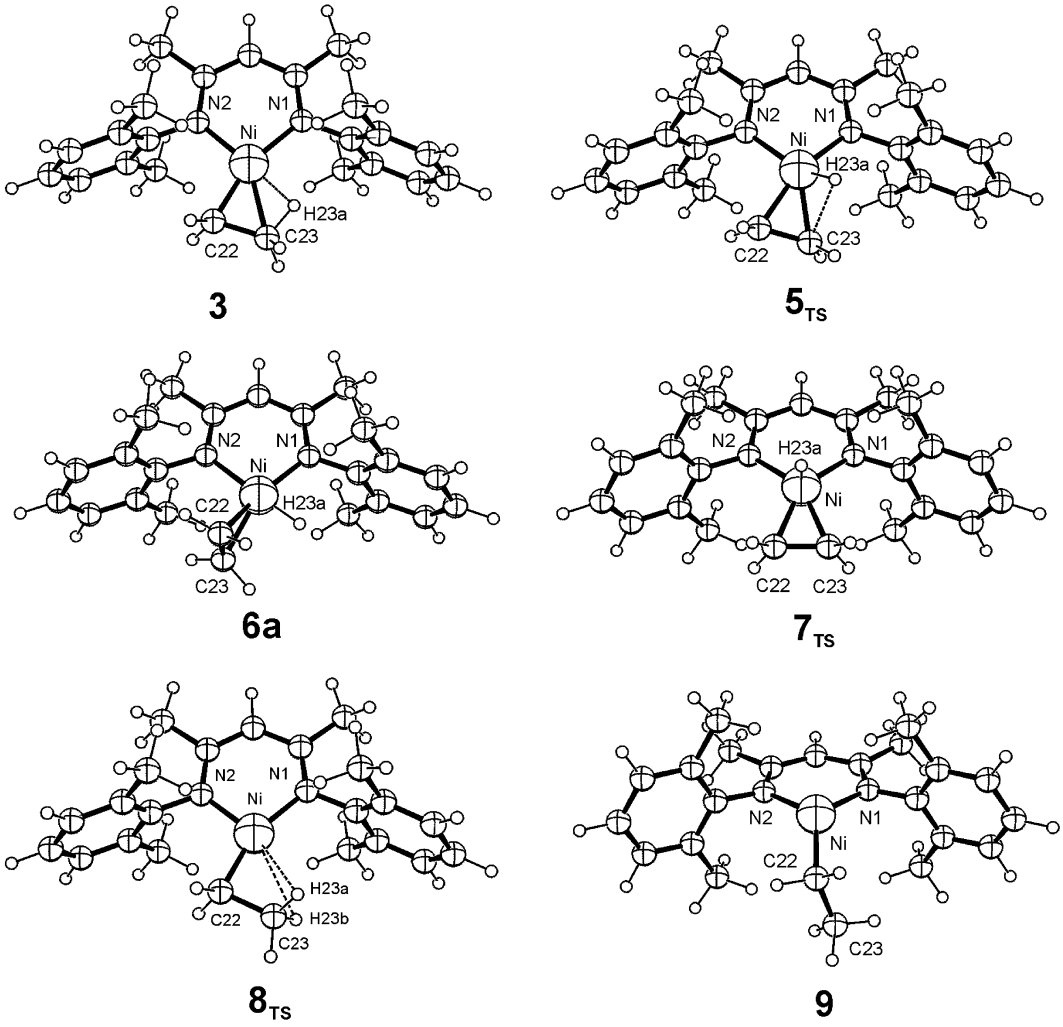

Figure 5. Three-dimensional representations of calculated structures **3**−**9**.

slight twist of about 5° between the N−Ni−N and C−Ni−C planes and the H23A atom is moved in the opposite direction, indicating only a weak β-C−H interaction (C23−H23A = 1.91 Å). In the resulting ethene−hydride complex **6a**, ethene is bound perpendicular to the plane containing the hydride and ancillary β-diketiminate ligands, the favored coordination mode for ethene in square-planar d^8 complexes.[58] The C22−C23 bond (1.39 Å) is somewhat longer than a regular C=C double bond, a result of π-back-bonding with the metal center. Now a nickel−hydride, the H23A atom is located in the square plane with a Ni−H bond distance of 1.44 Å. No structure of **6a** with an in-plane coordination of ethene[30,34] could be optimized. The transition state for the exchange of the ethene and the hydride ligand ($\mathbf{7_{TS}}$) could also be located. In the tetrahedral $\mathbf{7_{TS}}$, a significantly longer C23−H23A separation (2.29 Å) similar to that in the ethene−hydride ground state **6** (2.30 Å) was identified. We could also determine the barrier for the C−C bond rotation as $\Delta G^{\ddagger} = 7.5$

(58) Mingos, D. M. P. In *Comprehensive Organometallic Chemistry*; Wilkinson, G., Stone, F. G. A., Abel, E. W., Eds.; Pergamon Press: Oxford, 1982; Vol. 3, p 1.

Scheme 4. In-Plane Rotation of the β-CH_3 Group of **3** (B3LYP/6-31G (d) Free-Energy Values at 298.15 K/1 atm in Kilocalories per Mole)

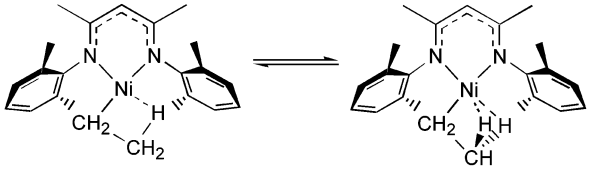

3 0.0 **8_{TS}** +7.5

kcal/mol at 298.15 K (Ni−C 2.39 Å; Ni−H 2.52 Å in the TS) (Scheme 4), which is in general agreement with the value of 8.5(5) kcal/mol estimated by VT NMR for **3**.

The free-energy barrier of the elimination calculated by DFT is 17.8 kcal/mol, a little higher than the experimentally determined value of 15.1(3) kcal/mol (from VT $^{13}C\{^1H\}$ NMR). The ethene−hydride ground-state species **6** is 14.4 kcal/mol higher in free energy compared to the β-agostic structure **3**. The reverse reaction (ethene insertion into the Ni−H bond) requires a free activation energy of only 3.4 kcal/mol. These computational results support the assumption of a β-H elimination/reinsertion mechanism for the symmetrization of the C_α and C_β atoms in variable temperature $^{13}C\{^1H\}$ NMR spectra of **3**. The observed exchange of both sets of H_α and H_β as well as C_α and C_β atoms in **3** is thus due to the perpendicular orientation of ethene relative to the Ni−H23A bond in the square plane of **6** so that reinsertion to reform **3** may occur in either direction with equal likelihood (C22−H23A and C23−H23A = 2.30 Å in **6**). According to our DFT calculations, the symmetrization process observed by ^1H NMR that interconverts the β-diketiminato methyl groups on opposite sides of the ancillary ligand in **3** could proceed via the tetrahedral $\mathbf{7_{TS}}$ for which an activation energy of 21.1 kcal/mol was determined. Thus, the activation energy for this symmetrization should be 3.3 kcal/mol higher in energy than that for H_α and H_β exchange. Despite many attempts, no symmetrization transition state for structure **3** which contains an orientation of the β-H agostic alkyl group perpendicular to that of the ground state could be optimized. Extrapolated from a related nickel complex with an anionic salicylaldimine ligand, where the activation energy of such a transition state was determined by 32.7 kcal/mol, the energy in our case should also be higher than 30 kcal/mol.[59] This pathway would therefore not be able to compete with those involving the lower-energy transition states $\mathbf{5_{TS}}$ and $\mathbf{7_{TS}}$.

Furthermore, the observation of no KIE in the symmetrization observed by ^1H NMR suggests a mechanism for this process other than reversible β-hydride elimination/reinsertion since the latter should show a significant k_H/k_D. The theoretically determined KIE at 298.15 K for $\mathbf{5_{TS}}$ is $k_H/k_D = 2.40$ ($\Delta G_H =$ 17.81 vs $\Delta G_D = 18.33$), while the corresponding value for $\mathbf{7_{TS}}$ is $k_H/k_D = 3.04$ ($\Delta G_H = 21.07$ vs $\Delta G_D = 21.73$).

We considered an additional pathway for the symmetrization observed by ^1H NMR that involves a change from the singlet ground state to a triplet excited state. Spin crossing processes are not appreciably affected by isotopic substitution[60−64] and therefore could lead to an indistinguishable KIE in this case. In a recent article, Holland et al. described some evidence for the low temperature formation of the related, three-coordinate nickel(II)−methyl complex LNiMe that employs bulkier *N*-aryl and backbone substituents on the β-diketiminate ancillary ligand.[65] The paramagnetically shifted ^1H NMR resonances attributed to the d^8 LNiMe suggest that it is a triplet. The DFT-optimized open-shell structure **9** (Figures 5 and 6) is somewhat pyramidal at Ni, possessing a tetrahedrally biased open coordination site (geometrical parameters in Table 1).

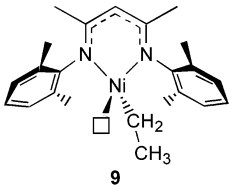

9 -0.8

Figure 6. Calculated structure of tetrahedrally biased triplet [Me_2NN]Ni(CH_2CH_3) (**9**). (B3LYP/6-31G (d) free-energy values at 298.15 K/1 atm in kilocalories per mole)

Coupled with the facile C−C bond rotation expected in a non-β-agostic ethyl group, movement of the Ni-bound ethyl group in either direction out of the square plane of **3** to form **9** is equally likely and thus could explain the symmetrization of each side of the β-diketiminato ligand observed in ^1H NMR spectra of **3**. We calculate almost no energy difference between the singlet state **3** and triplet state **9**. This small energetic difference suggests that interconversion of these electronic configurations should be facile. The barrier of the intersystem crossing for a simplified system was calculated to be $\Delta E =$ 12.3 kcal/mol, identified by the crossing point between the singlet and triplet surfaces. An Evans method measurement of **3** in benzene-d_6 shows that $\mu_{eff} < 0.1\ \mu_B$, suggesting that this excited state would be at least 2 kcal/mol higher in energy assuming the spin-only expected magnetic moment for the d^8 triplet state of ca. 2.8 BM.

The presence of two closely spaced but distinct β-diketiminato backbone C−H resonances in low temperature NMR spectra of the β-agostic propyl complex **4** indicates the presence of two isomers. At −79 °C in toluene-d_8 (500 MHz), the major isomer observed is the primary *n*-propyl **4a** that exhibits diastereotopic ^1H NMR signals at δ 0.22 and 0.00 ppm for the Ni−CH_2 group as a consequence of the γ-CH_3 group being held out of the square plane because of the β-H agostic interaction. The β-CH_2 resonances are broad but well-separated, appearing at δ −0.40 and −14.43 ppm corresponding to the nonagostic and agostic sites, respectively, while the γ-CH_3 group appears as a triplet at δ 0.59 ppm. Each set of α-CH_2 and β-CH_2 resonances coalesces with increasing temperature and gives rise to a triplet at δ 0.11 ppm and a broad signal at δ −7.4 (each of area 2), consistent with rapid interchange of the β-H atoms into and out of the agostic site. An activation barrier of 9.9(3) kcal/mol was calculated for this process at −60 °C.

Two resonances attributable to the Ni-bound isopropyl group in [Me_2NN]Ni($CHMe_2$) (**4b**) are also observed at −79 °C in the ^1H NMR spectrum (500 MHz) of **4**. A multiplet at δ 0.62 ppm and a broad resonance centered at δ −4.8 ppm are assigned to the α-CH and one β-Me group, respectively. We attribute

(59) Deubel, D. V.; Ziegler, T. *Organometallics* **2002**, *21*, 1603.

(60) Schröder, D.; Fiedler, A.; Ryan, M. F.; Schwarz, H. *J. Phys. Chem.* **1994**, *98*, 68.
(61) Fiedler, A.; Schröder, D.; Shaik, S.; Schwarz, H. *J. Am. Chem. Soc.* **1994**, *116*, 10734.
(62) Schröder, D.; Schwarz, H.; Clemmer, D. E.; Chen, Y.; Armentrout, P. B.; Baranov, V. I.; Böhme, D. K. *Int. J. Mass Spectrom. Ion Processes* **1997**, *161*, 175.
(63) Filatov, M.; Shaik, S. *J. Phys. Chem. A* **1998**, *102*, 3835.
(64) Schröder, D.; Shaik, S.; Schwarz, H. *Acc. Chem. Res.* **2000**, *33*, 139.
(65) Holland, P. L.; Cundari, T. R.; Perez, L. L.; Eckert, N. A.; Lachicotte, R. T. *J. Am. Chem. Soc.* **2002**, *124*, 14416.

Scheme 5. β-H Elimination/Reinsertion Reaction of **4a** (via $\mathbf{10_{TS}}$) to Give an Equilibrium with Branched Isomer **4b** (B3LYP/6-31G(d) Free-Energy Values at 298.15 K/1 atm in Kilocalories per Mole)

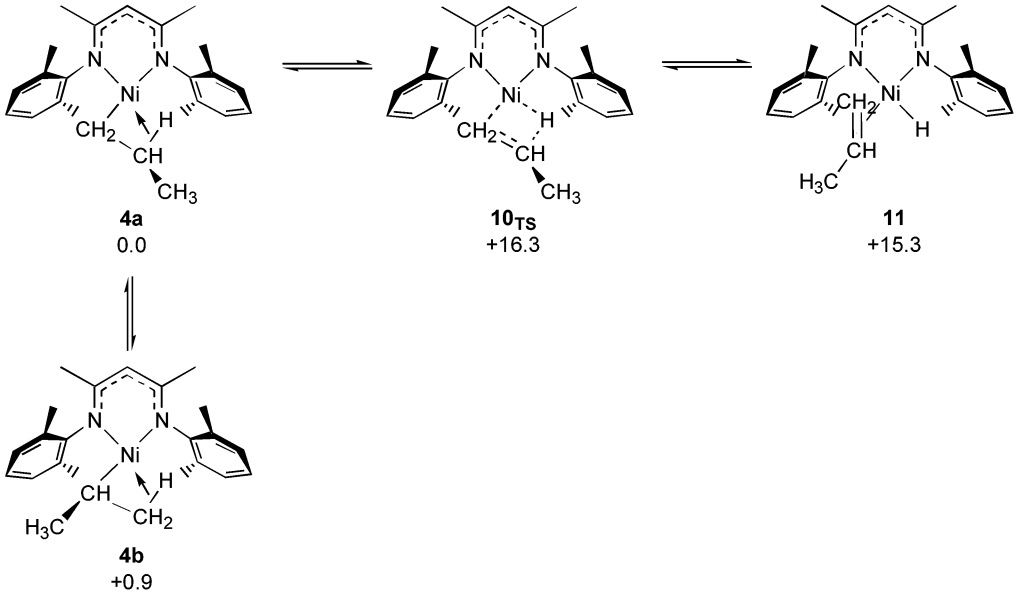

Table 2. Geometric Parameters (Å and deg) for Calculated Structures **4a**, **4b**, **10**−**12**[a]

	4a	4b	10_{TS}	11	12
Ni−N1	1.91 [1.882(2)]	1.91 [1.882(2)]	1.91	1.89	2.01
Ni−N2	1.85 [1.870(2)]	1.85 [1.870(2)]	1.95	1.97	1.96
Ni−C22	1.88 [1.900(4)]	1.89 [1.865(18)]	1.97	2.00	1.94
Ni−C23	2.14 [2.111(5)]	2.11 [2.66]	2.01	2.02	3.07
Ni−H23A	1.66 [1.61]	1.68	1.42	1.43	-
C23−H23A	1.16 [0.98]	1.15	2.09	2.25	-
C22−C23	1.49 [1.387(6)]	1.50	1.41	1.40	1.52
C23−C24	1.53 [1.544 (6)]	1.52 (C22−C24)	1.51	1.51	1.39 (C24−C25)
N1−Ni−N2	98.4 [97.49(10)]	98.0	95.9	95.5	93.4
Ni−C22−C23	77.8 [78.1(3)]	76.3	71.0	70.3	124.0
N2−Ni−C22−C23	−179.8 [−176.0]	−167.8	146.8	117.5	−100.9

[a] B3LYP/6-31G(d). Results from X-ray analysis of **4a** and **4b** are given in brackets. The X-ray structure of **4b** is not β-H agostic.

the upfield shift of the broad resonance to the rapid exchange of all H atoms of this β-Me group through an agostic site, though no specific β-H interaction was identified in the minor occupancy attributed to **4b** in the X-ray structure of **4**. Above 0° C, the broad resonance at δ −4.8 shifts to δ −2.7 ppm, indicating rapid rotation of all β-H atoms through the agostic site. Above 0 °C, interconversion between the primary and secondary alkyls **4a** and **4b** via reversible β-H elimination to form the propene−hydride intermediate **11** becomes significant on the NMR time scale (Scheme 5).

In contrast to that observed in related cationic Ni−diimine[26] and neutral anilinotroponate systems,[53] the secondary propyl **4b** lies somewhat higher in energy than the linear *n*-propyl ground state **4a** (Scheme 5). An equilibrium constant $K_{eq} = [\mathbf{4b}]/[\mathbf{4a}]$ may be determined over the temperature range 0−40 °C to give $\Delta H = +1.7(4)$ and $\Delta S = 5(1)$. Above 30 °C, the averaged β-agostic resonances in **4a** and **4b** at δ −2.7 and −7.4 ppm begin to broaden more appreciably and the α-CH_2 and γ-CH_3 resonances of **4a** coalesce, signaling rapid isomerization between **4a** and **4b** on the NMR time scale (Scheme 5). Curiously, the predicted equilibrium constant [secondary]/[primary] of 0.25 at the temperature at which **4** was crystallized (−35 °C) is very similar to the secondary/primary occupancy ratio of 0.22/0.78 = 0.28 observed in the X-ray structure of **4**.

Accordingly, calculations on the β-H elimination/reinsertion reaction were repeated for the linear β-agostic propyl complex **4a** (Scheme 5, geometric parameters in Table 2, three-dimensional respresentations in Figure 7). During the β-H elimination process involving **4a**, the bond lengths in the transition state $\mathbf{10_{TS}}$ are only slightly affected by the substitution by a methyl group as compared to that observed in $\mathbf{5_{TS}}$ for the corresponding ethyl analogue **3**. Steric interactions of the additional methyl group lengthen the C23−H23A bond distance in $\mathbf{10_{TS}}$ to 2.09 Å as compared to 1.91 Å in $\mathbf{5_{TS}}$, signifying that the transition state is located later on the reaction coordinate than that for **3**. The propene ligand in the β-H elimination product **11** is twisted from being perpendicular to the square plane by ca. 30°, a result of steric interactions with the β-diketiminato *N*-aryl groups. It should be noted that in an earlier DFT study of a cationic nickel diimine propene−hydride complex with less bulky *N*-substituents, the propene ligand was oriented perpendicular to the square plane.[32]

Consistent with the solution NMR characterization of **4a** and **4b**, we calculate the β-agostic branched propyl complex [Me_2-NN]Ni($CHMe_2$) (**4b**) to be somewhat higher in energy than the β-agostic linear complex [Me_2NN]Ni($CH_2CH_2CH_3$) (**4a**). The barrier for the β-H elimination transition state $\mathbf{10_{TS}}$ (16.3 kcal/mol) is comparable to that found for **3** (17.8 kcal/mol), although

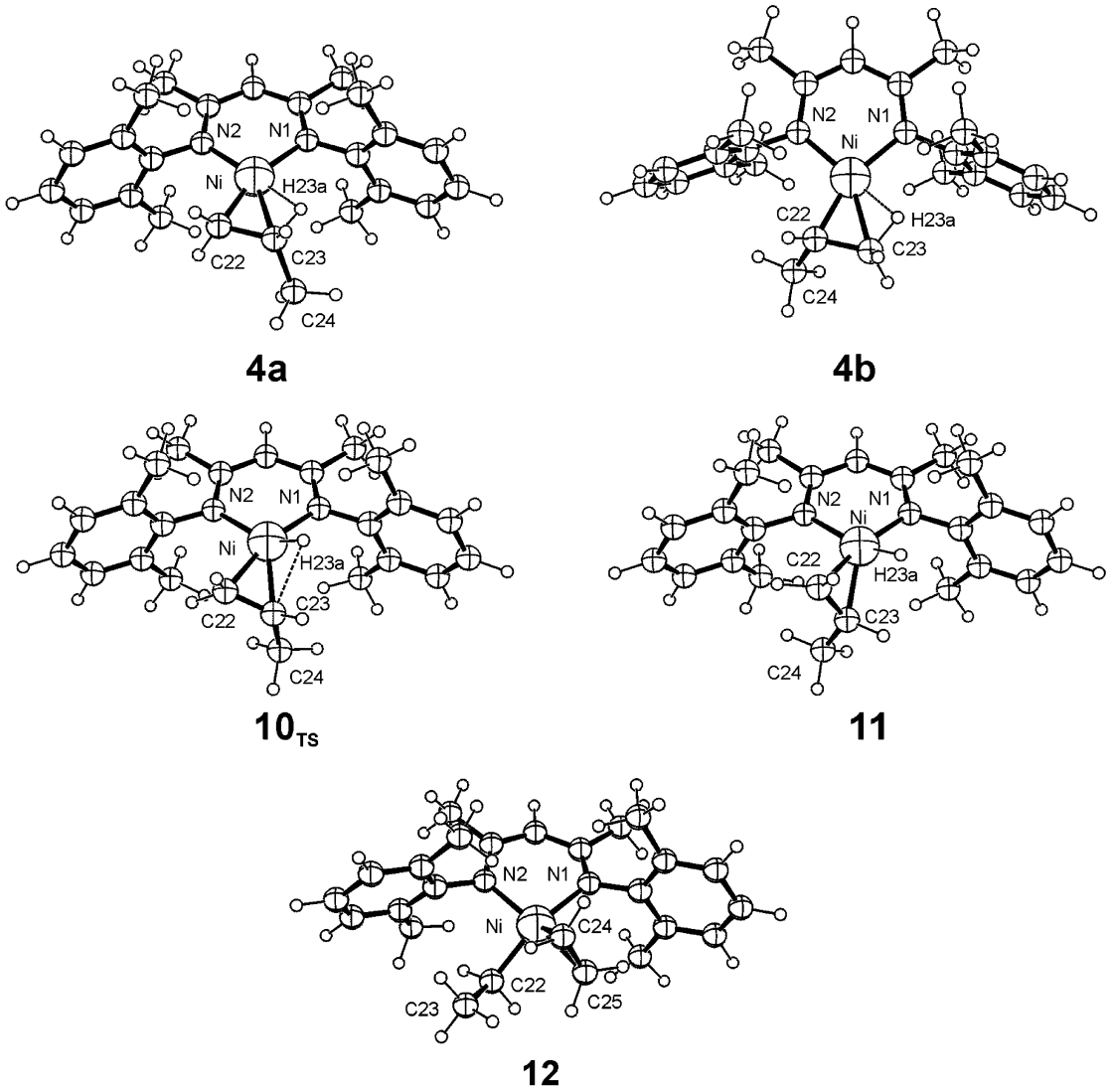

Figure 7. Three-dimensional representations of the calculated structures for **4a**, **4b**, and **10**−**12**.

Scheme 6. Reversible Ethene Coordination to **3** (B3LYP/6-31G* Free Energy at 298.15 K/1 atm in Kilocalories per Mole)

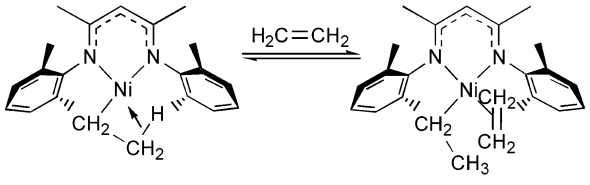

3 0.0 **12** +13.2

the corresponding propene−hydride **11** (+15.3 kcal/mol) is destabilized relative to the ethene−hydride **6** (+14.4 kcal/mol). This is likely a result of the distorted propene orientation, which leads to a poorer overlap of the ligand π-orbitals with the metal d-orbitals, weakening π-back-bonding.

Addition of 6 equiv of ethylene to β-agostic **3** at −50 °C results in the immediate formation of a new species in low concentration assigned as the ethylene adduct [Me_2NN]Ni(CH_2-CH_3)(η^2-CH_2CH_2) (**12**) (Scheme 6). The Ni−ethyl group in **12** is not β-agostic, shown by ^{1}H NMR resonances at δ 0.25 (α-CH_2) and δ 0.95 ppm (β-CH_3). Further warming results in an increase in the concentration of **12** at the expense of **3**. Although slow below 0 °C, ethylene insertion into the Ni−alkyl bond does occur in **12** to provide new species with broad, upfield ^{1}H resonances at −2.7 and −7.3 ppm. These new signals are assigned to primary and secondary Ni−alkyls that interconvert via β-H elimination/reinsertion and result in the formation of branched ethylene oligomers.[46]

DFT calculations on the ethene coordination reaction lead to an interesting result (Scheme 6, geometric parameters in Table 2; three-dimensional representation in Figure 7). Ethene coordination to **3** is slightly exothermic, but endergonic. As in ethene−hydride **6**, the ethene ligand in **12** adopts a perpendicular orientation relative to the square plane in a tetrahedrally distorted complex with the C24−C25 bond lengthened to 1.39 Å by π-back-bonding. The coordination of ethene to **3** is exothermic in electronic energy. From DFT calculations, ΔH remains approximately constant at −2.4 kcal/mol over the temperature range −50 to 25 °C. As expected, the coordination of ethene leads to a negative ΔS and results in a positive ΔG_{rxn} of +13.2 kcal/mol at 298.15 K (+10.4 kcal/mol at 243.15 K). Thus, **3** is the resting state of the oligomerization catalyst, and only low concentrations of the ethene−ethyl complex **12** should be present at room temperature with moderate ethene concentrations.

The dissociation reaction of lutidine in the ethyl−lutidine complex **1** and the corresponding thermodynamic isotope effect

Table 3. Geometric Parameters of the Calculated Structure **1** (B3LYP/6-31G(d)) and from the X-ray Analysis of **1**

	1 (calculated)	**1** (from X-ray)[46]
Ni−N1	2.00	1.987(3)
Ni−N2	1.94	1.915(3)
Ni−C1	1.96	1.965(4)
C1−C2	1.53	1.497(7)
Ni−N3	1.91	1.916(3)
N1−Ni−N2	93.4	93.16(12)
C1−Ni−N3	87.3	86.74(14)
Ni−C1−C2	124.0	119.9(3)

K_H/K_D of 1.3(2) was investigated by DFT methods (Scheme 1). Again the complex **1** was optimized without any simplifications (Becke3LYP/6-31G(d)). Important geometric parameters are given in Table 3. The DFT structure again shows good agreement with the solid-state structure. The calculated free energies at 298.15 K are −7.05 kcal/mol for **1** and −6.91 kcal/mol for **1**-d_5. This results in a theoretically determined K_H/K_D of 1.25, consistent with the experimental finding. The reason for this secondary kinetic isotope effect is the conversion of the terminal C−H bond to a β-agostic C−H bond. Because of interactions with the metal, the β-agostic C−H vibrational frequency is lower than that of the β-C−H bond in the open structure. This leads to a smaller zero-point energy difference of the isotopomers in structure **3** and, accordingly, to a smaller free-energy difference between nonagostic **1** and β-agostic **3**.

Conclusions

Chemical removal of 2,4-lutidine from solutions of [Me_2NN]Ni(R)(2,4-lutidine) (R = Et (**1**), Pr (**2**)) allows for the isolation of the base-free, neutral β-agostic species [Me_2NN]Ni(R) (R = Et (**3**), Pr (**4**)) that have been characterized by single-crystal X-ray as well as detailed solution and computational studies. Intermediate in structure between nonagostic monoalkyls and alkene−hydride complexes, the β-agostic complexes undergo facile β-H elimination/reinsertion for which an activation barrier $\Delta G^{\ddagger} = 15.1$ (3) kcal/mol was measured by VT $^{13}C\{^1H\}$ NMR for **3**. Both primary and secondary Ni−propyl groups are observed in the solid state and in solution for **4**, with the primary β-agostic Ni−$CH_2CH_2CH_3$ representing the ground state by a narrow margin. This observation stands in contrast to the secondary β-agostic Ni−$CH(CH_3)_2$ ground state identified for related cationic α-diimine and neutral anilinotroponate N∩O systems. This difference may be a consequence of the more compressed coordination wedge in the β-diketiminate system due to its larger bite angle (as compared to α-diimines) that brings the two bulky *N*-aryl substituents closer together. Furthermore, the tighter coordination wedge apparently coupled with strong donation by the monoanionic N∩N ancillary ligand favors pseudo three-coordinate β-agostic alkyls over four-coordinate alkyl−ethylene complexes. This leads to a β-H agostic monoalkyl resting state under modest ethylene pressures with a corresponding low TOF for ethylene oligomerization/polymerization than that observed in more active cationic and neutral systems that rest as alkyl−ethylene species.

Experimental Section

General Consderations. All experiments were carried out in a dry nitrogen atmosphere using an MBraun glovebox and/or standard Schlenk techniques. 4A molecular sieves were activated in vacuo at 180 °C for 24 h. Diethyl ether and tetrahydrofuran (THF) were first sparged with nitrogen and then dried by passage through activated alumina columns. Pentane was first washed to remove olefins, stored over $CaCl_2$, and then distilled before use from sodium/benzophenone. All deuterated solvents were sparged with nitrogen, dried over activated 4A molecular sieves, and stored under nitrogen. ^1H and ^{13}C NMR spectra were recorded on either a Mercury Varian 300 MHz spectrometer (300 and 75.4 MHz, respectively) or a Unity Varian 500 MHz spectrometer (500 and 125 MHz, respectively). All NMR spectra were indirectly referenced to TMS using residual solvent signals as internal standards. Elemental analyses were performed on a Perkin-Elmer PE2400 microanalyzer in our laboratories (Georgetown).

Unlabeled Grignard reagents and BF_3(etherate) were obtained from Aldrich and used as received. CD_3CD_2I and $CH_3{}^{13}CH_2I$ used in the preparation of labeled Grignard reagents were used as received from Cambridge Isotope Laboratories. [Me_2NN]Ni(CH_2CH_3)(2,4-lutidine) (**1**) and [Me_2NN]Ni($CH_2CH_2CH_3$)(2,4-lutidine) (**2**) were prepared according to literature procedures.[46] [Me_2NN]Ni(CD_2CD_3)(2,4-lutidine) (**1**-d_5) was prepared in a similar procedure as used for **1**, employing an ether solution of the labeled Grignard reagent CD_3CD_2MgI.

Computational Details. The DFT calculations were performed with Gaussian98.[66] The density functional hybrid model Becke3LYP[67−70] was used together with the valence double-ζ basis set 6-31G(d). No symmetry or internal coordinate constraints were applied during optimizations. All reported intermediates were verified as true minima by the absence of negative eigenvalues in the vibrational frequency analysis. Transition-state structures (indicated by **TS**) were located using the Berny algorithm[71] until the Hessian matrix had only one imaginary eigenvalue. The identity of all transition states was confirmed by animating the negative eigenvector coordinate with MOLDEN.[72] The crossing point between the singlet and triplet state of **9** was determined by a published procedure.[73]

Approximate free energies were obtained through thermochemical analysis of the frequency calculation, using the thermal correction to Gibbs free energy as reported by Gaussian98. This takes into account zero-point effects, thermal enthalpy corrections, and entropy. For the purpose of comparability all energies reported in this article, unless otherwise noted, are free energies at 298 K and have not been recalculated at the actual temperature of the experiment. Frequencies were scaled by 0.9806.[74] All transition states are maxima on the electronic potential energy surface. These may not correspond to maxima on the free-energy surface. We did not attempt to correct the free energy for hindered internal rotations.

Kinetic isotope effects were calculated from free-energy differences obtained from frequency calculations.

(66) Frisch, M. J.; Trucks, G. W.; Schlegel, H. B.; Scuseria, G. E.; Robb, M. A.; Cheeseman, J. R.; Zakrzewski, V. G.; Montgomery, J. A., Jr.; Stratmann, R. E.; Burant, J. C.; Dapprich, S.; Millam, J. M.; Daniels, A. D.; Kudin, K. N.; Strain, M. C.; Farkas, O.; Tomasi, J.; Barone, V.; Cossi, M.; Cammi, R.; Mennucci, B.; Pomelli, C.; Adamo, C.; Clifford, S.; Ochterski, J.; Petersson, G. A.; Ayala, P. Y.; Cui, Q.; Morokuma, K.; Malick, D. K.; Rabuck, A. D.; Raghavachari, K.; Foresman, J. B.; Cioslowski, J.; Ortiz, J. V.; Stefanov, B. B.; Liu, G.; Liashenko, A.; Piskorz, P.; Komaromi, I.; Gomperts, R.; Martin, R. L.; Fox, D. J.; Keith, T.; Al-Laham, M. A.; Peng, C. Y.; Nanayakkara, A.; Gonzalez, C.; Challacombe, M.; Gill, P. M. W.; Johnson, B. G.; Chen, W.; Wong, M. W.; Andres, J. L.; Head-Gordon, M.; Replogle, E. S.; Pople, J. A. *Gaussian 98*, revision A.7; Gaussian, Inc.: Pittsburgh, PA, 1998.
(67) Lee, C.; Yang, W.; Parr, R. G. *Phys. Rev. B: Condens. Matter* **1988**, *37*, 785.
(68) Vosko, S. H.; Wilk, L.; Nusair, M. *Can. J. Phys.* **1980**, *58*, 1200.
(69) Stephens, P. J.; Devlin, F. J.; Chabalowski, C. F.; Frisch, M. J. *J. Phys. Chem.* **1994**, *98*, 11623.
(70) Becke, A. D. *J. Chem. Phys.* **1993**, *98*, 5648.
(71) Peng, C.; Ayala, P.; Schlegel, H. B.; Frisch, M. J. *J. Comput. Chem.* **1996**, *17*, 49.
(72) Schaftenaar, G.; Noordik, J. H. *J. Comput.-Aided Mol. Des.* **2000**, *14*, 123.
(73) Harvey, J. N.; Aschi, M.; Schwarz, H.; Koch, W. *Theor. Chim. Acc.* **1998**, *99*, 95.
(74) Scott, A. P.; Radom, L. *J. Phys. Chem.* **1996**, *100*, 16502.

$$KIE = \frac{k_H}{k_D} = \exp\left[\frac{\Delta G_D - \Delta G_H}{RT}\right] \quad (1)$$

$$\Delta G_X = G_X^{\ddagger} - G_X^{\text{educts}} \quad X = H \text{ or } D \quad (2)$$

Determination of Thermodynamic Isotope Effect for 2,4-Lutidine Dissociation from [Me$_2$NN]Ni(CH$_2$CH$_3$)(2,4-lutidine) (1). A sample of [Me$_2$NN]Ni(CH$_2$CH$_3$)(2,4-lutidine) (0.050 g, 0.10 mmol) or [Me$_2$-NN]Ni(CD$_2$CD$_3$)(2,4-lutidine) (0.050 g, 0.10 mmol) was dissolved in 1.0 mL of toluene-d_8 in a volumetric flask and transferred into an NMR tube. Pentane was added as an internal standard. ^{1}H NMR spectra were acquired every 10 °C over the temperature range −40 to 50 °C. The integration of resonances corresponding to free (δ 8.38 ppm) and bound lutidine (δ 7.47 ppm) against the internal standard allowed the calculation of the equilibrium constant at a given temperature using the following dependence:

$$K_{eq} = \{[\text{free lutidine}]^2/[\text{bound lutidine}]\} \times [\text{initial concentration of } \mathbf{1} \text{ (or } \mathbf{1}\text{-}d_5)]$$

Van't Hoff plots of ln K_{eq} vs $1/T$ allowed the calculation of ΔH = 9.4(1.0) kcal/mol and ΔS = 23(4) cal/mol·K for lutidine dissociation from **1** (Figure S7) as well as ΔH = 8.3(7) and ΔS = 19(3) cal/mol·K for lutidine dissociation from **1**-d_5 (Figure S8), which leads to the thermodynamic isotope effect K_H/K_D = 1.3(2) at 25 °C.

Synthesis of [Me$_2$NN]Ni(CH$_2$CH$_3$) (3). A solution of BF$_3$(etherate) (0.085 g, 0.600 mmol) in 2 mL of Et$_2$O was added with stirring to a solution of [Me$_2$NN]Ni(CH$_2$CH$_3$)(2,4-lutidine) (0.300 g, 0.600 mmol) in 10 mL of Et$_2$O. The solution turned yellow immediately and became cloudy. The volatiles were removed in vacuo, and the yellow residue was triturated twice with 5 mL of pentane. The solid residue was then extracted with 10 mL of pentane, filtered through Celite, and concentrated to dryness. This pentane extraction/concentration cycle was carried out a total of three times. A final cycle was then performed in which the solution was concentrated to small volume (ca. 1 mL) and kept at −35 °C for 5 days. Tan crystals that formed were collected on a frit and dried in vacuo to afford 0.111 g (47%) of the product. ^{1}H NMR (toluene-d_8, −79 °C): δ 7.14, 7.06, 7.03, 7.01, 6.99, 6.96, 6.94, 6.91, 6.90, 6.87, 6.85, 6.63 (aromatic), 5.02 (s, 1, backbone-C-*H*), 2.46 (s, 6, *o*-CH$_3$), 2.41 (s, 6, *o*-CH$_3$), 1.54 (s, 3, backbone-CH$_3$), 1.51 (s, 3, backbone-CH$_3$), 0.08 (q, 2, NiC*H*$_2$CH$_3$), −1.03 (br, 2, NiCH$_2$C*H*$_2$H$_{agost}$), −14.11 (br, 1, NiCH$_2$CH$_2$*H*$_{agost}$). ^{13}C NMR (toluene-d_8, −40 °C): δ 159.01, 158.15, 155.44, 154.62, 130.67, 130.18, 128.50, 124.35, 123.90, 123.45, 97.01 (backbone-*C*-H), 22.18, 21.26, 19.13, 19.10, 16.12 ($J_{C\alpha-H}$ = 152.71), 1.32 ($J_{C\alpha-H}$ = 121.38). Anal. Calcd for $C_{23}H_{30}N_2$: C, 70.25; H, 7.71; N, 7.13. Found: C, 70.20; H, 7.90; N, 7.35.

Synthesis of [Me$_2$NN]Ni(C$_3$H$_7$) (4). A solution of BF$_3$(etherate) (0.145 g, 1.02 mmol) in 2 mL of Et$_2$O was added with stirring to a solution of [Me$_2$NN]Ni(CH$_2$CH$_2$CH$_3$)(2,4-lutidine) (0.526 g, 1.02 mmol) in 10 mL of Et$_2$O. The solution turned yellow immediately and became cloudy. The volatiles were removed in vacuo, and the yellow residue was triturated twice with 5 mL of pentane. The solid residue was then extracted with 10 mL of pentane, filtered through Celite, and concentrated to dryness. This pentane extraction/concentration cycle was carried out a total of three times. A final cycle was then performed in which the solution was concentrated to small volume (ca. 1 mL) and kept at −35 °C for several days. Tan crystals that formed were collected on a frit and dried in vacuo to afford 0.256 g (62%) of the product. ^{1}H NMR (toluene-d_8, −79 °C, primary isomer **4a**): δ 7.04−6.90 (aromatic), 5.03 (s, 1, backbone-C-*H*), 2.48 (s, 6, *o*-CH$_3$), 2.45 (s, 6, *o*-CH$_3$), 1.55 (s, 3, backbone-CH$_3$), 1.50 (s, 3, backbone-CH$_3$), 0.59 (br, 3, NiCH$_2$CH$_2$C*H*$_3$), 0.22 (br, 1, NiC*H*HCH$_2$CH$_3$), −0.003 (br, 1, NiCH*H*CH$_2$CH$_3$), −0.40 (br, 1, NiCH$_2$C*H*H$_{agost}$CH$_3$), −14.43 (br, 1, NiCH$_2$CH*H*$_{agost}$CH$_3$). ^{1}H NMR (toluene-d_8, −79 °C, secondary isomer **4b**): δ 7.04−6.90 (aromatic), 5.04 (s, 1, backbone-C-*H*), 2.60, 2.45, 2.37, 2.35, (s, 3, *o*-CH$_3$), 1.55, 1.51 (s, 3, backbone-CH$_3$), 0.62 (br, 1, NiC*H*(CH$_3$)$_{agost}$(CH$_3$), -0.40 (br, 3, NiCH(CH$_3$)$_{agost}$(C*H*$_3$)), −4.8 (v br, 3, NiCH(C*H*$_3$)$_{agost}$(CH$_3$). ^{13}C NMR (toluene-d_8, −79 °C): δ 158.85, 158.49, 157.58, 155.76, 155.01, 154.16, 152.77, 131.31, 130.99, 130.12, 129.81, 129.74, 129.05, 128.34, 128.22, 128.15, 124.06, 123.74, 123.63, 97.55 (backbone-*C*-H **4b**), 97.23 (backbone-*C*-H **4a**), 24.62, 23.99, 23.17, 22.37, 21.55, 21.17, 19.54, 19.35, 19.18, 19.15, 18.54, 15.67, 14.93. Anal. Calcd for $C_{24}H_{32}N_2$: C, 70.79; H, 7.92; N, 6.88. Found: C, 70.37; H, 8.31; N, 7.25.

Determination of Barrier to β-H Elimination/Reinsertion for [Me$_2$NN]Ni(CH$_2$CH$_3$). ^{13}C-labeled Grignard reagent (prepared from CH$_3$^{13}CH$_2$I) was used to prepare mono ^{13}C-labeled [Me$_2$NN]Ni(CH$_2$-CH$_3$)(2,4-lutidine) (**1**-^{13}C). ^{13}C{^{1}H} NMR spectra of **1**-^{13}C indicated equal incorporation of the ^{13}C-label into the C$_\alpha$ and C$_\beta$ positions. Mono ^{13}C-labeled [Me$_2$NN]Ni(CH$_2$CH$_3$) (**3**-^{13}C) was prepared following an analogous procedure for **3**. Coalescence of the ^{13}C{^{1}H} (75.4 MHz) resonances at δ 16.12 (C$_\alpha$) and 1.32 (C$_\beta$) ppm (from the low temperature limit) at 75(3) °C leads to $\Delta G^{\ddagger}$ = 15.1(3) kcal/mol at this temperature.

Determination of ΔH and ΔS for Equilibrium between 4a and 4b. ^{1}H NMR spectra of a toluene-d_8 solution of **4** were taken at 10° intervals between 0 and 40 °C. The unitless equilibrium constant K_{eq} = **4b**/**4a** was determined by integration of the Ni−C*H*$_2$CH$_2$CH$_3$ signal of **4a** at δ 0.11 ppm (relative area 2) against the backbone C−H resonance at δ 5.04 ppm that corresponds to both **4a** and **4b** (each relative area 1). The mole fraction χ_{4a} could thus be directly determined, from which $K_{eq} = 1 - \chi_{4a}/\chi_{4a}$. A van't Hoff plot (see Supporting Information) allowed the determination of ΔH = +1.7(4) kcal/mol and ΔS = 5(1) cal/mol·K.

Addition of Ethylene to [Me$_2$NN]Ni(CH$_2$CH$_3$) (3). A sample of [Me$_2$NN]Ni(CH$_2$CH$_3$) (0.046 g, 0.117 mmol) was dissolved in 1.0 mL of toluene-d_8 in a volumetric flask and transferred into an NMR tube. Mesitylene (0.007 g, 0.06 mmol) was added as an internal standard. Approximately 6 equiv of ethylene at 1 atm was added by syringe at −78 °C, and a ^{1}H NMR spectrum was acquired at −50 °C. In addition to resonances for **3** and free ethylene at δ 5.28 ppm, a new species in low concentration with a nonagostic ethyl group was observed at δ 0.95 (t, 3, Ni−CH$_2$C*H*$_3$) and 0.25 (q, 2, Ni−C*H*$_2$CH$_3$) ppm assigned to [Me$_2$NN]Ni(CH$_2$CH$_3$)(η^2-CH$_2$CH$_2$) (**12**). The bound ethylene ligand of **12** is likely obscured by *N*-aryl Me resonances. An equilibrium constant could be estimated at this temperature by integration of normalized resonances corresponding to free ethylene (δ 5.28 ppm), [Me$_2$NN]Ni-(CH$_2$CH$_3$)(η^2-CH$_2$CH$_2$) (δ 0.25 ppm) as well as the β-agostic [Me$_2$-NN]Ni(CH$_2$CH$_3$) (δ 0.08 ppm) against an internal standard (mesitylene): K_{eq} = {[**12**]/[**3**][free ethylene][initial concentration of **3**] = 0.45 M^{-1} (at −50 °C). Followed by ^{1}H NMR, insertion of ethylene at higher temperatures led to linear (δ −7.3 ppm) and branched (δ −2.7 ppm) β-agostic Ni−alkyl groups.

X-ray Structure Refinement Details. Single crystals of **3** and **4** were mounted under mineral oil on glass fibers and immediately placed in a cold nitrogen stream at −90(2) °C on a Bruker SMART CCD system. Full spheres of data were collected (0.3° ω-scans; $2\theta_{max}$ = 56°; monochromatic Mo Kα radiation, λ = 0.7107 Å) and integrated with the Bruker SAINT program. Structure solutions were performed using the SHELXTL/PC suite[75,76] and XSEED.[77] Intensities were corrected for Lorentz and polarization effects, and an empirical absorption correction was applied using Blessing's method as incorporated into the program SADABS.[78] With the exception of the Ni−ethyl and Ni−propyl groups in **3** and **4**, respectively, non-hydrogen atoms were refined with anisotropic thermal parameters and hydrogen atoms were included in idealized positions. Tables of all atomic

(75) *SHELXTL-PC*, version 5.10; Bruker Analytical X-ray Services: Madison, WI, 1998.
(76) Sheldrick, G. M. *SHELX-97*; Universität Göttingen: Göttingen, Germany, 1997.
(77) (a) Barbour, L. J. *J. Supramol. Chem.* **2001**, *1*, 189. (b) *XSEED* Home Page, http://xseed.net.
(78) (a) Sheldrick, G. M. *SADABS*, version 2.01; Bruker-Analytical X-ray Services: Madison, WI, 1999. (b) Based on the method described in: Blessing, R. H. *Acta Crystallogr., Sect A.* **1995**, *51*, 33.

coordinates, anisotropic thermal parameters, and complete bond lengths and bond angles are included as Supporting Information.

In the initial refinement of **3**, elongated anisotropic thermal ellipsoids of C22 and C23 perpendicular to the C−C bond suggested disorder in the Ni−ethyl group, which was modeled with two sets of positions in a 83:17 ratio. C22A/C22A and C22B/C23B were refined anisotropically, though thermal parameters within each pair of C atoms were constrained to be similar. The initial refinement of **4** similarly suggested disorder in the Ni−propyl group. After lowering the occupancy of the Ni−propyl C atoms of the β-agostic linear isomer **4a** (C22A−C24A) and isotropically refining them, we identified three new peaks corresponding to the C atoms of the isopropyl isomer **4b** in the Fourier difference map. These peaks assigned as C22B−C24B were allowed to isotropically refine against C22A−C24A after constraining their isotropic thermal parameters to be similar to those of C22A−C24A. Fixing the occupancy ratio (**4a**/**4b** = 78:22), releasing the thermal parameter constraint, and anisotropically refining C22A−C24A and C22B−C24B (anisotropic parameters of sets of atoms C22A−C24A and C22B−C22B lightly constrained to be similar) led to a reduction of R_1 [$I > 2\sigma(I)$] from 5.29% to 4.29% with a concomitant reduction in the maximum absolute peak height from 0.89 $e^-/Å^3$ to 0.57 $e^-/Å^3$. Because of the low occupancy of minor isomer **4b** (22%), the unconstrained C−C distances within the isopropyl group (1.39(2) and 1.66(3) Å) are not realistic. Nonetheless, this conformation would be nonagostic even if they assumed a more normal value (e.g., C23A−C24A = 1.544(6) Å).

Acknowledgment. T.H.W. is grateful to Georgetown University for startup funding as well as the NSF CAREER program (No. 0135057) for partial support of this work. E.K. thanks Dr. Angel deDios for assistance in obtaining high field NMR spectra. T.S. thanks the Leibniz Computer Center, Munich for computer time.

Supporting Information Available: VT ^{1}H NMR spectra for **3** and **4**, van't Hoff plots for loss of lutidine from **1** and **1-*d*$_5$** as well as the equilibrium between **4a** and **4b**, contour plots of the frontier molecular orbitals of **3**, tables of X-ray refinement data, bond distances, and bond angles along with fully labeled ORTEP plots for **3** (major and minor occupancies), **4a**, and **4b** (also provided in CIF format). This material is available free of charge via the Internet at http://pubs.acs.org.

JA0477221